New Method for Enhanced Efficiency in Detection of Gravitational Waves from Supernovae Using Coherent Network of Detectors

S. Mukherjee, L. Salazar*, J. Mittelstaedt†, O. Valdez
Center for Gravitational Wave Astronomy, Department of Physics,
The University of Texas Rio Grande Valley, One West University Boulevard, Brownsville, TX 78520‡

Supernovae in our universe are potential sources of Gravitational Waves (GW) that could be detected in a network of GW detectors like LIGO and Virgo. Core-collapse supernovae are rare, but the associated gravitational radiation is likely to carry profuse information about the underlying processes driving the supernovae. Calculations based on analytic models predict GW energies within the detection range of the Advanced LIGO detectors, out to tens of Mpc for certain types of signals e.g. coalescing binary neutron stars. For supernovae however,the corresponding distances are much less. Thus, methods that can improve the sensitivity of searches for GW signals from supernovae are desirable, especially in the advanced detector era. Several methods have been proposed based on various likelihood-based regulators that work on data from a network of detectors to detect burst-like signals (as is the case for signals from supernovae) from potential GW sources. To address this problem, we have developed an analysis pipeline based on a method of noise reduction known as the Harmonic Regeneration Noise Reduction (HRNR) algorithm. To demonstrate the method, sixteen supernova waveforms from the Murphy et al. 2009 catalog have been used in presence of LIGO science data. A comparative analysis is presented to show detection statistics for a standard network analysis as commonly used in GW pipelines and the same by implementing the new method in conjunction with the network. The result shows significant improvement in detection statistics.

PACS numbers: 95.85.Sz,04.80.Nn, 07.05.Kf, 02.50.Tt, 02.60.Pn

I. INTRODUCTION

Supernovae (SN) in our universe are potential sources of Gravitational Waves (GW) [1–3] that could be detected in a network of GW detectors. Several GW detectors are in operation, e.g., like LIGO [4], Virgo [5], and GEO600 [6]. Core-collapse supernovae are rare, but the associated gravitational radiation is likely to carry profuse information about the underlying processes driving the supernovae. Calculations based on analytic models predict GW energies within the detection range of the Advanced LIGO [14] detectors, out to tens of kpc.

Analysis of the GW signal of the post-bounce evolution of core-collapse supernovae using relativistic, two-dimensional explosion models have been calculated [19] . The waveforms show the accelerated mass motions associated with the characteristic evolutionary stages, which were also seen in previous studies [18, 20]. The basic model is that a quasi-periodic modulation by prompt post-shock convection is followed by a phase of relative quiescence. Following this, the amplitudes grow again due to violent hydrodynamical activity caused by convection and the standing accretion shock instability. Finally, a high-frequency, low-amplitude variation from proto-neutron star convection below the neutrinosphere appears superimposed on the low-frequency trend associated with the aspherical expansion of the SN shock after the onset of the explosion. The GW frequency from neutrino driven core collapse supernovae is expected to evolve from approximately100 Hz to about 1000 Hz.

Since the signals from these sources are weak, methods that can improve the sensitivity of searches for GW signals from SN are desirable, especially in the advanced detector era. Several methods have been proposed [15–17] based on various likelihood-based regulators that work on data from a network of detectors to detect burst-like signals (as is the case for signals from supernovae) from potential GW sources. To address this problem, we have developed and implemented a new technique of noise reduction in the supernova search pipeline based on Harmonic Regeneration Noise Reduction (HRNR) algorithm [21, 23–25]. The method is based on a multi-stage, high accuracy spectral estimation to effectively achieve higher signal to noise ratio (snr).

The paper is organized as follows. Section II to V describes the algorithm development in detail. Section VI describes the analysis pipeline where sixteen supernova waveforms from the Murphy et al. 2009 catalog [18] have been used in presence of LIGO science data. A comparative analysis is presented to show detection statistics for a standard network analysis as commonly used in GW pipelines and the same by implementing the new method in conjunction with the network. Section VII discusses the results and section VIII summarizes the conclusion.

*Current address: Information Technology Department, University of Texas Rio Grande Valley
†Supported by NSF Research Experience for Undergraduates grant at the University of Texas Rio Grande Valley in 2014; permanent address: Department of Physics, University of Chicago, 5720 S. Ellis Avenue, Chicago, IL 60637
‡Corresponding author:soma.mukherjee@utrgv.edu

II. METHOD

Noise reduction can be viewed as an estimation problem, where an unknown signal is to be estimated in the presence of noise, where only the noisy observation is available. We achieve noise reduction by exploiting the spectral diversity between the signal and the noise, along with the high degree of the nonstationarity of the signal. Consequently, it is natural to perform enhancement in the frequency domain.

We assume that the data segments used in the analysis satisfy assumptions of wide-sense stationarity (WSS) [7, 8].

Let us first establish some basic definitions.

In general, a WSS process $x(t)$ is a weak form of stationary process in which the first and the second moments dont vary significantly with respect to time. In other words the mean is constant, i.e.

$$E[x(t)] = \mu(x(t)) = \mu(x(t+\tau)), \forall\tau. \tag{1}$$

The correlation function depends only on the difference between two time instances, i.e.

$$\begin{aligned} E[x(t_1)x(t_2)] = R_x(t_1,t_2) &= R_x(t_1+\tau, t_2+\tau) \\ &= R_x(t_1-t_2, 0), \forall\tau, t_1, t_2 \end{aligned} \tag{2}$$

We will now write the Discrete Fourier Transform (DFT) coefficients as $X(p,k)$. Thus, $|X(p,k)|$ is the amplitude spectrum. Here, k is the frequency bin index and p is the time frame (or segment) index. The variance of the signals DFT coefficients is given by $\sigma^2_{XX}(p,k) = E(|X(p,k)|^2)$. The periodogram is defined as $\frac{1}{K}|X(p,k)|^2$, where K is the length of each time frame. The power spectral density (psd) is defined as $P_{XX}(p,k) = \frac{1}{K}E(|X(p,k)|^2)$, for $K \to \infty$.

The basic problem can be stated as follows. We assume an additive noise model.

$$x_p(t) = s_p(t) + n_p(t) \tag{3}$$

where $x(t)$ is the data stream, $s(t)$ is the signal, embedded in noise $n(t)$. Here t denotes the discrete time index of the segement p.

Because of the linearity of the fourier transform, the noise model is expressed in the frequency domain as

$$X(p,k) = S(p,k) + N(p,k). \tag{4}$$

Here $X(p,k)$, $S(p,k)$ and $N(p,k)$ are DFT coefficients obtained at frequency index k and time frame p for noisy data, signal and noise respectively. It is reasonable to assume that S and N are independent. Therefore, the correlation between them is zero, i.e.

$$E[S(p,k)N(p,k)] = 0, \quad \forall k, p. \tag{5}$$

This is reasonable because the only statistical property we assume is that it is uncorrelated with noise. Thus, the relation between the corresponding psd's is given by

$$P_{XX}(p,k) = P_{SS}(p,k) + P_{NN}(p,k). \tag{6}$$

Our aim is to find an estimator $\tilde{S}(p,k)$ of the signal from the noisy observed data $X((p,k)$ such that expectation value of distortion between the true signal and its estimate based on spectral noisy features is minimized. In other words, the estimate $\tilde{S}(p,k)$ of the signal is a function (denoted by $\mathcal{F}$) of all three quantities - signal psd, noise psd and the observed data,

$$\widehat{S}(p,k) = \mathcal{F}(P_{NN}(p,k), P_{SS}(p,k), x(p,k)). \tag{7}$$

This is further developed in more explicit details later in this section through equations [12-15].

Since we do not have a unique spectral estimate, we begin by estimating the snr from the noisy data.

An estimate of $S(p,k)$ is then obtained by applying a spectral gain $\Gamma(p,k)$ to each short-time spectral component $X(p,k)$. The choice of the distortion measure determines the gain behavior, i.e., the tradeoff between noise reduction and signal distortion. However, the key parameter is the estimated snr because it determines the efficiency of the signal enhancement for a given noise psd. The most widely accepted definition of the snr [35] in the GW literature is given by

$$snr = [4\int_0^\infty df \frac{|\tilde{s}(f)|^2}{(N(f))}]^{\frac{1}{2}}. \tag{8}$$

Here, $N(f)$ is the one-sided psd of the noise and $\tilde{s}(f)$ is the fourier transform of GW time domain data $s(t)$.

In keeping with the general definition of the snr, which is the ratio of the signal power to the noise power, at this point, for convenience in further derivation, we will make a slight change in notation by introduction of two parameters: the *a posteriori* snr and the *a priori* snr, *respectively defined by*

$$snr_{post}(p,k) = \frac{|X(p,k)|^2}{P_{NN}(p,k)} \tag{9}$$

and

$$snr_{priori}(p,k) = \frac{P_{SS}(p,k)}{P_{NN}(p,k)}. \tag{10}$$

We also define the instantaneous *snr as follows.*

$$\begin{aligned} snr_{ins}(p,k) &= \frac{|X(p,k)|^2 - P_{NN}(p,k)}{P_{NN}(p,k)} \\ &= snr_{post}(p,k) - 1. \end{aligned} \tag{11}$$

$snr_{ins}(p,k)$ is taken as a measured estimate of the local *a priori* snr in a spectral subtraction approach [10]. We would like to note that the *a priori* and *a posteriori* are not used in a Bayesian sense, but rather to denote the previous and subsequent data segments in the analysis.

In reality, $P_{NN}(p,k)$ and $P_{SS}(p,k)$ are both unknown and need to be estimated. $P_{NN}(p,k)$ can be estimated by

the classical minimum statistics methods [11, 23]. This method provides a good estimate of psd even in presence of nonstationarity of noise. The method involves tracking spectral minima in each frequency band and minimization of a mean square estimation error (MMSE) in each time step. Specifically, if we describe $\chi_1, \chi_2, \chi_3, \ldots, \chi_n$ as the minima in the frequency bands, we can make an estimate of $P_{NN}(p,k)$ in the following way. Let $P'_{NN}(p,k)$ represent such an estimator of $P_{NN}(p,k)$. The error in the above estimate is

$$\varepsilon(\mathbf{X}) = P_{NN}(p,k) - P'_{NN}(p,k). \tag{12}$$

Since ε is a random variable, $E\{|\varepsilon|^2\}$ represents the mean square error. Under the MMSE, the best estimator for $P_{NN}(p,k)$ is given by the conditional mean

$$P'_{NN}(p,k) = E[P_{NN}(p,k)|\chi]. \tag{13}$$

This leads to an optimal unbiased smoothed estimate of the spectral density.

After this, the spectral gain is obtained as follows.

$$\Gamma(p,k) = f(\widehat{snr}_{priori}(p,k), \widehat{snr}_{post}(p,k)). \tag{14}$$

The function f is chosen in this case to be a Wiener filter [34] described below. The signal estimate can then be obtained as follows.

$$\widehat{S}(p,k) = \Gamma(p,k)X(p,k) \tag{15}$$

A. Wiener filter

The Wiener filter is based on the MMSE between the estimated signal and the true signal. The basic assumption here is that the s_p and n_p are jointly WSS with known covariance functions $R_s(p)$, $R_n(p)$ and $R_{sn}(p)$. The aim of the process is to estimate s_p as a function of x by finding the linear MMSE estimate of s_p based on x_p.

Let us consider a finite impulse response (FIR [26]) filter of length $N+1$.

$$\hat{s}_p = \sum_{m=p-N}^{p} h_{p-m}x_m = \sum_{j=0}^{N} h_j x_{p-j}. \tag{16}$$

The coefficients h_j need to be calculated such that the MMSE is achieved.

In order to acheive this, let us first determine the optimal condition equation (i.e. the expanded error equation).

$$\epsilon = E\left(\sum_{k=-\infty}^{+\infty} h[k]x[n-k] - s[k]\right)^2. \tag{17}$$

The value that minimizes ϵ can the be obtained by setting $\frac{\partial \epsilon}{\partial h[m]} = 0$ for all values of m except when $h[m] = 0$.

$$\frac{\partial \epsilon}{\partial h[m]} = E\left[\left(2\sum_k h[k]x[n-k] - s[k]\right)s[n-m]\right] = 0. \tag{18}$$

Denoting $2\sum_k h[k]x[n-k] - s[k] = e$, the above equation indicates that

$$R_{es}[m] = E\left[e[n]s[n-m]\right] = 0 \ \ \forall m. \tag{19}$$

Thus, the error is orthogonal or uncorrelated to all data used to form the optimal estimate. It may be noted here that

$$\begin{aligned} R_{es}[m] &= E\left[e[n]s[n-m]\right] \\ &= E\left[(\hat{x}[n] - x[n])s[n-m]\right] \\ &= R_{\widehat{xs}}[m] - R_{xs}[m]. \end{aligned} \tag{20}$$

In other words, the orthogonality principle can also be stated as

$$R_{\widehat{xs}}[m] = R_{xs}[m]. \tag{21}$$

To find the actual values of $h[n]$, the following relation is used.

$$R_{\widehat{xs}}[m] = h[m] * R_{ss}[m] = R_{xs}[m]. \tag{22}$$

An equivalent way to state this is

$$\sum_k h[k]R_{ss}[m-k] = R_{sx}[m]. \tag{23}$$

The above equation is a set if linear equations that needs to be solved for the values of $h[n]$. For a filter of length N+1, there are N+1 equations of N+1 vaues of $h[n]$. In matrix form, these equations can be written as

$$\begin{pmatrix} R_{ss}[0] & R_{ss}[-1] & \ldots & R_{ss}[N] \\ R_{ss}[1] & \ldots & \ldots & \ldots \\ \ldots & \ldots & \ldots & R_{ss}[-1] \\ R_{ss}[N] & \ldots & R_{ss}[1] & R_{ss}[0] \end{pmatrix} \begin{pmatrix} h_0 \\ \ldots \\ \ldots \\ h_N \end{pmatrix} = \begin{pmatrix} R_{xs}(0) \\ \ldots \\ \ldots \\ R_{xs}(N) \end{pmatrix}.$$

In a compact form, h is given by

$$h = R_s^{-1}R_{xs}. \tag{24}$$

These are the Yule-Walker equations [12]. It is noted that $R_x \geq 0$. The matrix on the left is a Toeplitz matrix, i.e.constant along the diagonals. They can be solved by Levinson-Durbin [13] methods that are standard applications in software packages like the Matlab [32].

The MMSE can now be computed as follows [9]:

$$E[(\hat{s}_p - s_p)^2] = R_{ss}[0] - h^T R_{xs}. \tag{25}$$

B. How to find $\Gamma(p,k)$: Relation between *local a priori* and *local a posteriori* snr

In order to obtain a mathematical form of the estimate of $\Gamma(p,k)$, we would derive the relation between the *a priori* and *a posteriori* snr by following an approach developed in [22].

Assuming the model given in equation [3], the amplitude of the noisy signal is given by,

$$|X(p,k)| = \left(|S(p,k)|^2 + |N(p,k)|^2 + 2|S(p,k)||N(p,k)|cos\beta(p,k)\right)^{\frac{1}{2}} \tag{26}$$

where $\beta(p,k)$ is the phase angle between $S(p,k)$ and $N(p,k)$.

Assuming that we now have some knowledge of the signal and noise from equation [13] and [15], let us define a *local a priori* and *a poteriori* snr as follows.

$$snr_{post}^{local}(p,k) = \frac{|X(p,k)|^2}{|N(p,k)|^2} \tag{27}$$

and

$$snr_{priori}^{local}(p,k) = \frac{|S(p,k)|^2}{|N(p,k)|^2} \tag{28}$$

Using equation [26] in equation [27], we get

$$snr_{post}^{local}(p,k) = 1 + snr_{priori}^{local}(p,k) + 2\sqrt{snr_{priori}^{local}(p,k)} \times cos\beta(p,k) \tag{29}$$

For Wiener filter, $snr_{post}(p,k)$ is assumed to be equal to $1 + snr_{priori}(p,k)$. This implies that the phase difference is constant, or, $\beta(p,k) = \pi/2$ or, the signal and the noise add in quadrature. This is also already seen in section II.

III. INFORMATION FROM THE PREVIOUS TIME FRAME: THE DECISION DIRECTED APPROACH

A. Principle

One of the most commonly used methods to obtain an estimator is known as the 'decision directed' (DD) [24, 25] approach. The DD estimator combines the estimated amplitude of the previous time frame and the noisy amplitude of the current frame under analysis into one estimator of the signal spectrum. Using the noise psd, the *a priori* and *a posteriori* snrs are computed as follows.

$$\widehat{snr}_{post}(p,k) = \frac{|X(p,k)|^2}{P_{NN}(p,k)} \tag{30}$$

and

$$\widehat{snr}_{priori}^{DD}(p,k) = \epsilon\frac{|\tilde{S}(p-1,k)|^2}{P_{NN}(p,k)} + (1-\epsilon)P[\widehat{snr}_{post}(p,k) - 1] \tag{31}$$

where $\tilde{S}(p-1,k)$ stands for estimated signal spectrum at the previous frame and $P[\widehat{snr}_{post}(p,k) - 1)]$ is the half wave rectification (HWR). The HWR in this case implies that the maximum relative to zero, is taken into account.$P[.]$ or the HWR has the following properties.

$$\begin{aligned} P[x'] &= x' \;\; if \; x' \geq 0 \\ P[x'] &= 0 \;\; \text{otherwise.} \end{aligned} \tag{32}$$

This is made to ensure that the result is not negative. ϵ is chosen to be 0.98. The above estimate is the DD estimate [25]. The estimator is obtined by combining equations [14] and [15].The main idea here is that the signal amplitude is estimated from the $(p-1)^{th}$ frame instead of the amplitude itself in the p^{th} frame. It is so named because $\widehat{snr}_{priori}^{DD}(p,k)$ is updated on the basis of the previous signal amplitude estimate.

With the spectral gain being chosen as the Wiener filter [34], we have

$$\Gamma_{DD}(p,k) = \frac{\widehat{snr}_{priori}^{DD}(p,k)}{1 + \widehat{snr}_{priori}^{DD}(p,k)} \tag{33}$$

Derivation of equation 31 is given in detail in [25].

B. Consequences

Two observations are important here: (i) when the instantaneous snr is $>> 0$, $snr_{priori}(p,k)$ corresponds to a frame delayed version of the instantaneous snr; (ii) when the instantaneous snr is < 0 or $= 0$, $snr_{priori}(p,k)$ corresponds to a highly smoothed and delayed version of instantaneous snr. These two effects are observed from equation [11]. This means that the variance of the *a priori* snr is reduced compared to the instantaneous snr. The direct effect of this phenomenon is the reduction of underlying noise to effectively enhance the signal [24]

However, it may be noted that the delay inherent to the DD algorithm can be a drawback especially in the beginning and end of the signal. Furthermore, this delay introduces a bias in gain estimation which limits noise reduction performance.

To explain this effect more, let us consider that a signal appears in frame p. Thus, *a priori* snr is zero in frame $(p-1)$. In the current frame, we have

$$\widehat{snr}_{priori}^{DD}(p,k) = (1-\epsilon)P[\widehat{snr}_{post}(p,k) - 1)]. \tag{34}$$

Thus, from equation [10], the estimated *a priori* snr is the attenuated version of the instantaneous snr, the attenuation factor being $(1-\epsilon)$. If the phase factor $\beta(p,k)$ in equation [31] is $\frac{\pi}{2}$,

$$\widehat{snr}^{local}_{priori}(p,k) = [\widehat{snr}_{post}(p,k)-1] = \widehat{snr}^{local}_{ins}(p,k). \quad (35)$$

In the case that the signal ends in a frame, the *a priori* snr may be overestimated. In this case, the second term in equation [31] is zero, leading the estimate to have a non-zero value determined by the first term. However, a null value is desired. Thus the signal spectrum may be overestimated.

IV. OVERCOMING THE OVERESTIMATION PROBLEM: TWO STEP NOISE REDUCTION TECHNIQUE USING INFORMATION FROM A LATER FRAME

In order to avoid some of the problems faced in the estimation of the *a priori* snr, a two step noise reduction (TSNR) technique has been developed. The DD algorithm introduces a frame delay when ϵ is ~ 1. As a result of this, the spectral gain matches the values in the p^{th} and the $(p-1)^{th}$ frame. We now adopt a two step approach by applying the DD algorithm to the $(p+1)^{th}$ frame too. In this approach, we first calculate spectral gain as given by equation [33]. In the next step, this gain is used to calculate the *a priori* snr in the $(p+1)^{th}$ frame. The gain factor is given by

$$\widehat{snr}^{TSNR}_{priori}(p,k) = \widehat{snr}^{DD}_{priori}(p+1,k). \quad (36)$$

Hence,

$$\widehat{snr}^{TSNR}_{priori}(p,k) = \frac{|\Gamma_{DD}(p,k)X(p,k)|^2}{P_{NN}(p,k)}. \quad (37)$$

It is possible to write this step by putting the weight factor in equation [31] equal to 1. Finally, the spectral gain is calculated as follows.

$$\Gamma_{TSNR}(p,k) = \frac{\widehat{snr}^{TSNR}_{priori}(p,k)}{1+\widehat{snr}^{TSNR}_{priori}(p,k)} \quad (38)$$

and hence the enhanced signal estimate is

$$\hat{S}(p,k) = \Gamma_{TSNR}(p,k)X(p,k). \quad (39)$$

As before, we have taken the chosen spectral gain to be the Wiener filter [34].

To summarize, the TSNR algorithm improves the noise reduction performance since the gain matches to the current frame whatever the snr.

To understand the improvement more clearly, the following is observed: (i) when the instantaneous snr is $>> 0$, $snr^{TSNR}_{priori}(p,k)$ corresponds to the instantaneous snr without any delay as was found in the DD approach. Further, as the $\widehat{snr}_{ins}(p,k)$ increases or decreases (corresponding to onset and offset of the signal), the response of the $snr^{TSNR}_{priori}(p,k)$ is also instantaneous, unlike the DD estimator; (ii) when the instantaneous snr is < 0 or $= 0$, $snr^{TSNR}_{priori}(p,k)$ is reduced more compared to the DD estimator.

A. Theoretical explanation

If no signal is present in the $(p-1)^{th}$ frame,

$$\hat{S}(p-1,k) = 0. \quad (40)$$

At the p^{th} frame, the DD approach gives the estimation for *a priori* snr as

$$\widehat{snr}^{DD}_{priori}(p,k) = (1-\epsilon)P(\widehat{snr}_{post}(p,k)-1). \quad (41)$$

When refining the *a priori* snr in the TSNR technique, according to equation [31],

$$\widehat{snr}^{TSNR}_{priori}(p,k) = \left[\frac{(1-\epsilon)P(\widehat{snr}_{post}(p,k)-1)}{1+(1-\epsilon)P(\widehat{snr}_{post}(p,k)-1)}\right]^2 \times snr_{post}(p,k). \quad (42)$$

By comparing equations [41 and 42] to search for the intersection of the curves defined by these equations, we find that

$$\widehat{snr}_{post}(p,k) > \frac{1}{2\epsilon}\left[1+2\epsilon+\sqrt{\frac{1+3\epsilon}{1-\epsilon}}\right] \quad (43)$$

It is evident from the above equation that the TSNR method delivers a greater signal power than the DD algorithm. Consequently, if a signal component appears abruptly at frame p , thus increasing the *a posteriori* snr, the estimated *a priori* snr tends to the *a posteriori* snr suppressing the bias introduced by the DD approach. This bias decreases when the *a posteriori* snr increases. However, if signal is absent at frame p too, keeping the *a posteriori* snr to a low level, the estimated *a priori* snr becomes lower than for the DD approach further limiting the noise.

Looking at the other extreme case, where *a priori* snr is higher in $(p-1)^{th}$ frame than in the p^{th} frame (i.e. the signal decays rapidly), the following approximation can be done.

$$\widehat{snr}^{DD}_{priori}(p,k) \sim \epsilon\widehat{snr}_{ins}(p-1,k) \quad (44)$$

The spectral gain is then approximated as follows.

$$\Gamma_{DD}(p,k) = \frac{\epsilon\widehat{snr}_{ins}(p-1,k)}{1+\epsilon\widehat{snr}_{ins}(p-1,k)} \quad (45)$$

Moreover, it is reasonable to assume that $\widehat{snr}_{ins}(p-1,k)$ 1 and is much greater than 1 and $\epsilon \sim 1$, equation [39] becomes

$$\Gamma_{DD}(p,k) \sim 1. \tag{46}$$

Inducting this approximation in [31] leads to

$$\begin{aligned} \widehat{snr}^{TSNR}_{priori}(p,k) &\sim \widehat{snr}_{post}(p,k) \\ &\sim \widehat{snr}_{ins}(p,k). \end{aligned} \tag{47}$$

The TSNR method leads to suppresion of *a priori* snr overestimation.

V. HARMONIC REGENERATION NOISE REDUCTION

The output signal from the previous step may still suffer some distortion due to estimation errors that may be present. It is very difficult to obtain a 100 % reliable spectral estimate and hence some errors are expected to remain. Most of the distortion happend due to loss of some harmonics. The Harmonic Regeneration Noise Reduction (HRNR) consists of applying a nonlinear function to the time signal enhanced in the process described in the previous section. The restored signal is given by

$$s_{rectified}(t) = \Phi(\tilde{s}(t)), \tag{48}$$

where Φ is the nonlinear function.The maximum value relative to zero (i.e. HWR) has been used in this case.

It is important to note that the $S_{rectified}(t)$ are created at the same positions as the original signal, thus *no distortions are produced*. Moreover, it contains a useful information that leads to a further refinement in the *a priori* snr estimate as follows.

$$\begin{aligned} \widehat{snr}^{HRNR}_{priori}(p,k) = &\frac{1}{P_{NN}(p,k)} \times (\Delta(p,k)|\tilde{s}(p,k)|^2 \\ &+(1-\Delta(p,k))|s_{rectified}(p,k)|^2). \end{aligned} \tag{49}$$

The $\Delta(p,k)$ is a mixing parameter.

$$0 \leq \Delta(p,k) \leq 1. \tag{50}$$

Mixing is important at this stage because the nonlinear function Φ is able to restore the harmonics lost due to spectral estimation error. Δ should meet the following conditions: When $\tilde{S}(p,k)$ provided by the TSNR method is reliable, Δ is equal to 1; if the estimate is not a reliable one, $\Delta(p,k) = 0$. A standard value, e.g. 0.5, can also be used in some cases. We will use

$$\Delta(p,k) = \Gamma_{TSNR}(p,k), \tag{51}$$

to meet the required conditions.

The refined *a priori* snr from equation [43] is now used to calculate the new spectral gain *with preservation of all features of the original signal*. As before, we have chosen the spectral gain to be the Wiener filter. Thus,

$$\Gamma_{HRNR}(p,k) = \frac{\widehat{snr}^{HRNR}_{priori}(p,k)}{1+\widehat{snr}^{HRNR}_{priori}(p,k)}. \tag{52}$$

At the final stage, the desired signal spectrum is given by,

$$\tilde{\mathbf{S}}(p,k) = \Gamma_{HRNR}(p,k)X(p,k) \tag{53}$$

A. Theoretical explanation of HRNR

As stated in the previous section, we choose the nonlinear function Φ as follows.

$$s_{rectified}(t) = Max[\hat{s}(t),0] = \hat{s}(t) \times \rho(\hat{s}(t)), \tag{54}$$

where ρ is defined as

$$\begin{aligned} \rho(g) &= 1 \ \text{ if } \ g > 0 \\ \rho(g) &= 0 \ \text{ if } \ g < 0. \end{aligned} \tag{55}$$

In other words, we have chosen the HWR. $\rho(g)$ defines an elementary repetitive waveform. It is reasonable to assume that, over a short time period, the signal is quasistationary. The fourier transform (FT) of $\rho(g)$ is given by,

$$\tilde{\rho}(\hat{s}(t)) = \frac{1}{T}\sum_{n=-\infty}^{\infty} Q(\frac{n}{T})\delta(\nu - \frac{n}{T}), \tag{56}$$

where δ is the Dirac delta function and ν denotes the frequency. $Q(\frac{n}{T})$ is the FT of the underlying elementary waveform at discrete frequency $\frac{n}{T}$. Using [56], the FT of $s_{rectified}(t)$ is given by,

$$\begin{aligned} \tilde{S}_{rectified}(t) = FT(\hat{s}(t)) \times \frac{e^{-i\theta}}{T} \\ \times \sum_{n=-\infty}^{\infty} Q(\frac{n}{T})\delta(\nu - \frac{n}{T}). \end{aligned}$$

θ is the phase angle at the origin. In summary, the spectrum of the rectified signal is the convolution between the signal enhanced by the TSNR and a harmonic comb with the same frequency as the signal. The method is remarkably simple and useful. Moreover, $\tilde{\rho}(\tilde{s}(t))$ rapidly decreases as $|n|$ increases, ensuring that regeneration takes place only using information from its near neighbors.

VI. ANALYSIS

A. Data used

Sixteen supernova waveforms from the Murphy et al. 2009 catalog [18] have been used in presence of LIGO fourth science run (S4 [27]) data for demonstration of results from the search algorithm. The catalog describes the GW signals from neutrino driven core collapse supernovae. The waveforms used in the study are shown in figure 1 and figure 2.

The analysis pipeline is shown in figure 3.

Sets of test data, each 60 seconds long, from the main GW channel (DARM_ERR) from two Hanford detectors (4 km arm-length H1 and 2 km arm-length H2) and the Livingston detector (4 km arm-length L1) are used for demonstration of results. Data streams have been injected with the signal waveforms. The signals are introduced in the data streams starting at 20 seconds after start. After this, data conditioning is applied to the data containing the signal. The data conditioning consists of the following steps. (i) Extraction of raw GW channel data with SN signals injected; let this time series be noted by T_0; (ii) Whitening T_0 [29] and dynamically removing [30, 31] the narrowband noise present in T_0; The resulting time series is denoted by T_0'; (iii) Filtering T_0' with a bandwidth of 50 Hz and 2048 Hz; The resulting time series is denoted by $filt_{T_0'}$; (iv) Re-sampling $filt_{T_0'}$ to represent the appropriate band- width.

The conditioned data sets are then applied to the input of the TSNR+HRNR denoising stage. The denoised output from the TSNR+HRNR module is then used as the input to a network analysis based on regularized maximum likelihood [15–17, 28].

B. Detection statistics

It is known that the detector response to GW signal is a linear combination of the unknown polarization waveforms $h_+(t)$ and $h_\times(t)$ arriving from a direction with polar angle θ_0 and azimuthal angle ϕ_0 in an earth-centered, ecliptic reference frame [28]

The output of the network algorithm for a given sky location θ_0 and azimuthal angle ϕ_0 , is the value of the likelihood of the data maximized over all possible $h_+(t)$ and $h_\times(t)$ waveforms. A skymap [15–17, 28]. is said to be constructed with the maximum likelihood values obtained as a function of θ_0 and azimuthal angle ϕ_0. The detection statistic is constructed from the skymap as follows.

$$R_{rad} = [(\frac{max_{\theta_0,\phi_0}\mathbf{S}(\theta_0,\phi_0)}{max_{\theta_0,\phi_0}\mathbf{S_0}(\theta_0,\phi_0)} - 1)^2 + (R_{mm} \times \frac{min_{\theta_0,\phi_0}\mathbf{S_0}(\theta_0,\phi_0)}{max_{\theta_0,\phi_0}\mathbf{S_0}(\theta_0,\phi_0)} - 1)^2]^{\frac{1}{2}}, \quad (58)$$

where R_{mm} is given by

$$R_{mm} = \frac{max_{\theta_0,\phi_0}\mathbf{S}(\theta_0,\phi_0)}{min_{\theta_0,\phi_0}\mathbf{S}(\theta_0,\phi_0)}, \quad (59)$$

and $\mathbf{S_0}$ is the expectation value of $\mathbf{S}$ when no signal is present in the data. R_{rad} is known as the radial statistics. It denotes the radial distance of the observed values in the $(R_{mm}, max_{\theta_0,\phi_0}\mathbf{S}(\theta_0,\phi_0)$ plane from the mean location in absence of the signal. The larger the radial distance, the higher is the detection probability.

VII. RESULTS

Figures 4 and 5 show the analysis results for one of the catalog waveforms (grw_12_2; progenitor mass 12, electron neutrino luminosity 2.2) injected into the data stream with a scale factor of 30, i.e. the original signal was multiplied by a scale of 30. Figure 4 shows the signal strength injected into the detector noise. For reference, a scale factor of 30 corresponds to the snr threshold below which the signal is not discerned in the network analysis radial distance statistics without the application of the TSNR+HRNR denoising module. Figure 5 top row shows the spectrograms of the signal+noise data after being conditioned without the TSNR+HRNR denoising effect (left panel) and the same with the inclusion of the TSNR+HRNR denoising (right panel.) It is clear even visually that the TSNR+HRNR denoising effectively has enhanced the snr of the embedded signal. The bottom row shows the radial statistics (as given in equation [36]) for the analysis performed without the proposed denoising (left panel) and with the TSNR+HRNR denoising (right panel.) In the first case, the max value of R_{rad} is around 0.4, while in the second case, it is about 5.5, an improvement of a factor of 14. It may be noted that the noise scatter is much less in the second case than the first one.

Figures 6-9 show the core of analysis results. These plots correspond to the 16 Murphys waveforms that have been analyzed. The progenitor masses varied from 12 to 40 with various luminosity values between 1.8 and 13.0. The x-axis represents distance in kpc and the y-axis reprsents the detection snr defined from equation [59]. The detection snr is equal to the average value of the radial distance R_{rad} subtracted from the maximum value of the same that corresponds to the event detected. The lower curve (in blue) is the operating characeristic for the original pipeline without the implementation of the proposed TSNR+HRNR denoising module. The upper curve (in red) represents the same with the incorporation of the TSNR+HRNR denoising. As can be seen, for all the 16 waveforms, the detection snr is higher across the distances for the combined HRNR+TSNR pipeline. It must be noted that at this stage, the actual values of the distances are not of any physical significance because we have used data from S4 just for demonstration of the method's efficiency.

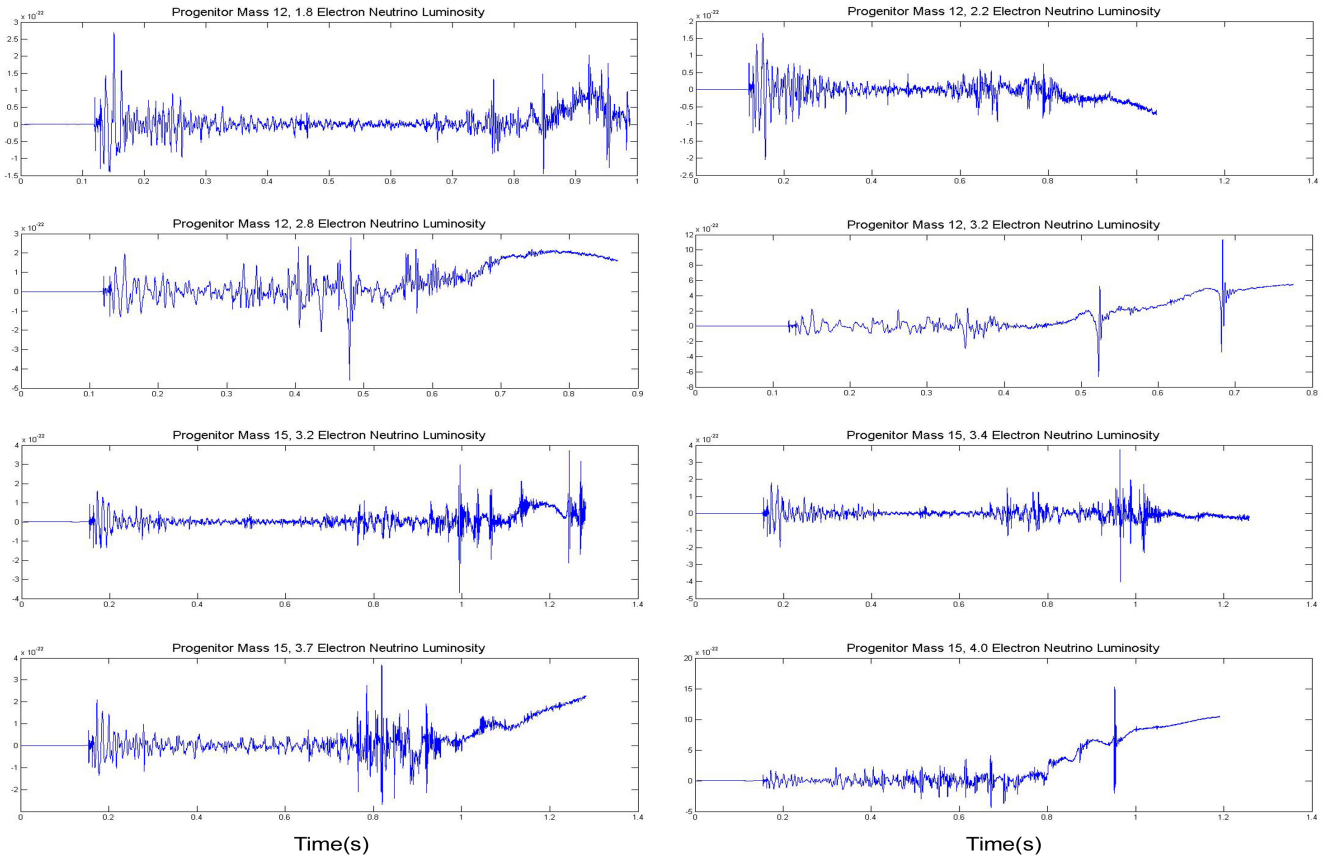

FIG. 1: The figure shows 8 supernovae waveforms used in the study from Murphy et. al. 2009 catalog [18] with progenitor masses 12 and 15.

A companion paper has been prepared with results from more recent science runs. More extensive testing has been performed with sine-gaussian, Murphy, long-bar, rotating core collapse (Dimmermeier [36]) waveforms by integrating this method to existing coherent wave burst (cWB)-based [33] supernova search pipeline. More supernova signals will be incorporated in the study. It will indeed be interesting to note if the improvement in detection statistics noted in this study also remains persistent in the future studies as the advanced LIGO [14] comes into operation.

VIII. CONCLUSION

The result shows improvement in detection statistics (as defined and described in detail in section VI B) by a factor of up to 10 even for very weak snr. The improvement in the detection statistics grows steadily with increasing signal strengths. HRNR works robustly even with non-stationary, non-gaussian noise. A major advantage of the proposed method is that it is a stand-alone MATLAB [32] code module that can be easily plugged in to existing search pipelines without having to make alterations. HRNR contains adjustable parameters that can in principle improve the results even more.

As mentioned above, more extensive testing with S6 data has been performed with five different families of supernova waveforms by integrating this method to existing coherent waveburst supernova search pipeline. Receiver operating characteristics (ROC) and Coherent event displays (CED) are being generated for comparison. It will indeed be interesting to note if the improvement in detection statistics noted in this study also remains persistent in the future studies as the advanced LIGO [14]. With the direct observation of the first gravitational waves [37], this scenario presents an exciting possibility.

IX. ACKNOWLEDGMENT

This work is supported by NSF award number NSF PHY 1205585 (2012).Use of LIGO fourth science run

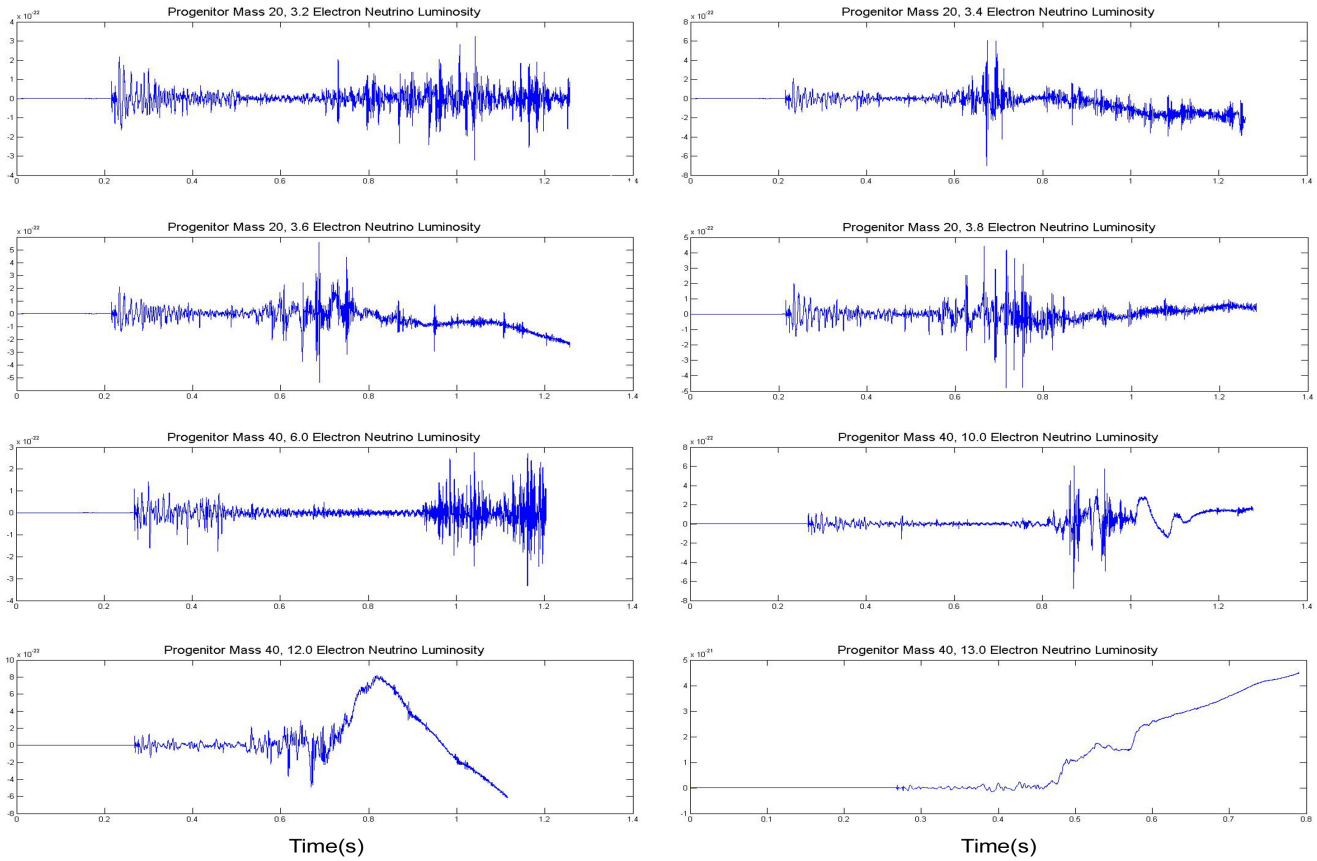

FIG. 2: The figure shows 8 supernovae waveforms used in the study from Murphy et. al. 2009 catalog [18] with progenitor masses 20 and 40.

data is acknowledged. Many thanks to Dr. Michele Zanolin for a careful reading of the manuscript.

[1] C. D. Ott, E. Abdikamalov, E. O'Connor, C. Reisswig, R. Haas, P. Kalmus, S. Drasco, A. Burrows, E. Schnetter, Correlated Gravitational Wave and Neutrino Signals from General-Relativistic Rapidly Rotating Iron Core Collapse, Phys. Rev. D. 86, 024026, 2012

[2] Christian D. Ott, Christian Reisswig, Erik Schnetter, Evan O'Connor, Ulrich Sperhake, Frank Lffler, Peter Diener, Ernazar Abdikamalov, Ian Hawke, and Adam Burrows, Dynamics and Gravitational Wave Signature of Collapsar Formation, Phys. Rev. Lett., 106, 161103, 2011

[3] Ernazar Abdikamalov, Christian D. Ott, Luciano Rezzolla, Luc Dessart, Harald Dimmelmeier, A. Marek, and H.-T. Janka, Axisymmetric General Relativistic Simulations of the Accretion-Induced Collapse of White Dwarfs, Phys. Rev. D. 88, 044012, 2010

[4] A. Abramovici, W. Althouse, R. Drever, Y. Gursel, S. Kawamura, F. Raab, D. Shoemaker, L. Sievers, R. Spero, K. Thorne, R. Vogt, R. Weiss, S. Whitcomb, and M. Zucker. Science, 256:325333, 1992.

[5] T. Accadia, F. Acernese, F. Antonucci, et al., Status and perspectives of the Virgo gravitational wave detector, Journal of Physics: Conference Series 203, 2010

[6] H. Grote, K. Danzmann, K.L. Dooley, R. Schnabel, J. Slutsky, H. Vahlbruch First Long-Term Application of Squeezed States of Light in a Gravitational-Wave Observatory, Phys. Rev. Lett. 110, 181101, 2013

[7] S. Kay, Fundamentals Of Statistical Signal Processing, vol. 1, Prentice Hall, London, 2001.

[8] S. Kay, Fundamentals Of Statistical Signal Processing, vol. 2, Prentice Hall, London, 2001.

[9] J. G. Proakis and M. Salehi, Digital Communications, 5th edition, McGraw-Hill College, 2007

[10] J. S. Lim and A. V. Oppenhein, Enhancement and bandwidth compression of noisy speech, Proc. IEEE, 67, pp. 1586-1604, 1979

[11] R. Martin, Noise power spectral density estimation based on optimal smoothing and minimum statistics, Proc. IEEE transactions on speech and audio, 9, 2001

[12] Weitian Chen, Brian D.O. Anderson, Manfred Deistler andAlexander Filler, Solutions of Yule-Walker equations for singular AR processes, Journal of Time Series Anal-

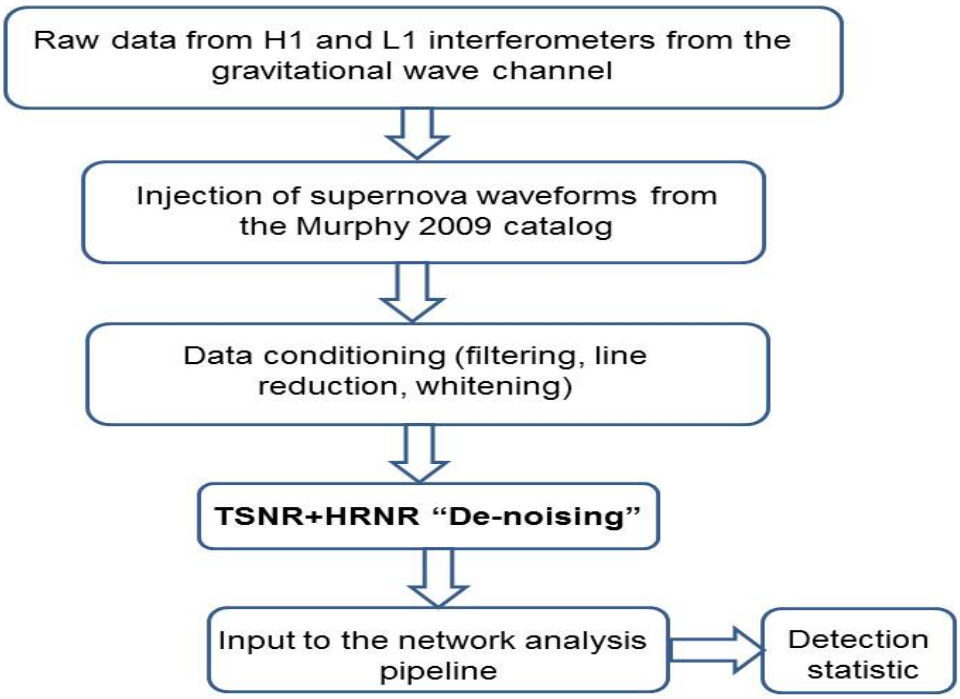

FIG. 3: The analysis pipeline starts with obtaining the raw data from three LIGO detectors (H1: Hanford 4k and L1: Livingstion 4k.) Supervovae signals are added to the data stream. The prepared data streams are now subjected to the data conditioning step where data are bandpassed between 50 Hz and 2048 Hz and all narrowband noise in this range is suppressed. The conditioned data now passes through the TSNR and HRNR module. The output from this module is supplied as the input to the network analysis pipeline. The network analysis pipeline yields the detection statistics in accordance with equations 58 and 59.

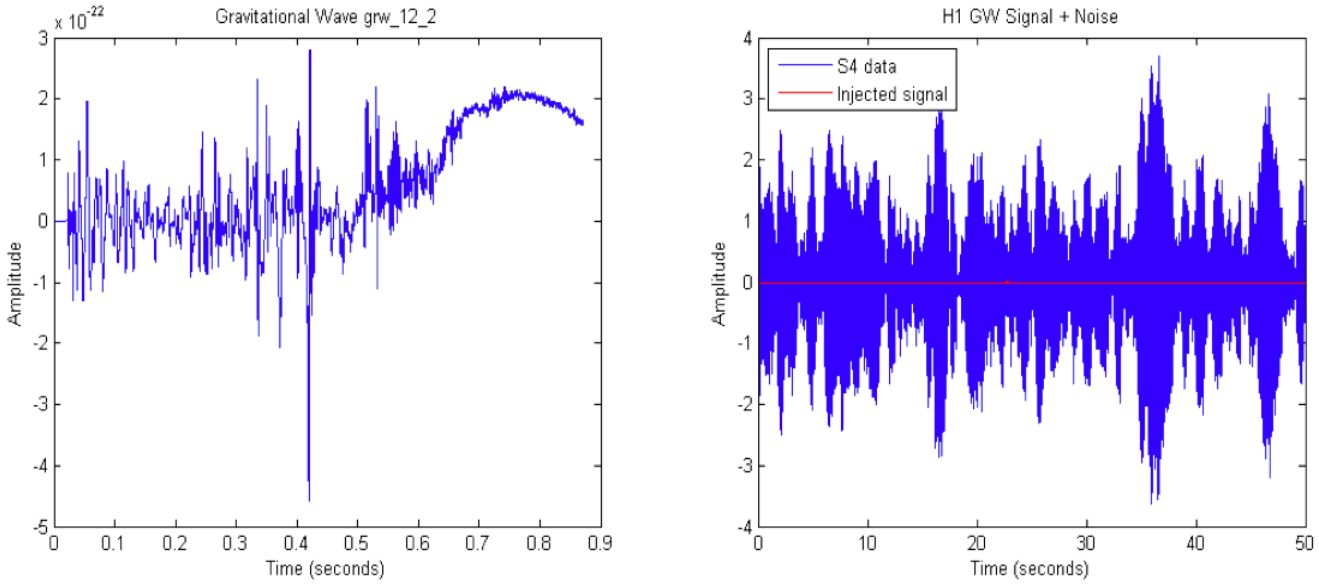

FIG. 4: The waveform (grw_12_2 , left panel) is injected into the data stream (right panel) with a scale factor of 30. The x-axis represents time in seconds and the y-axis is the amplitude.

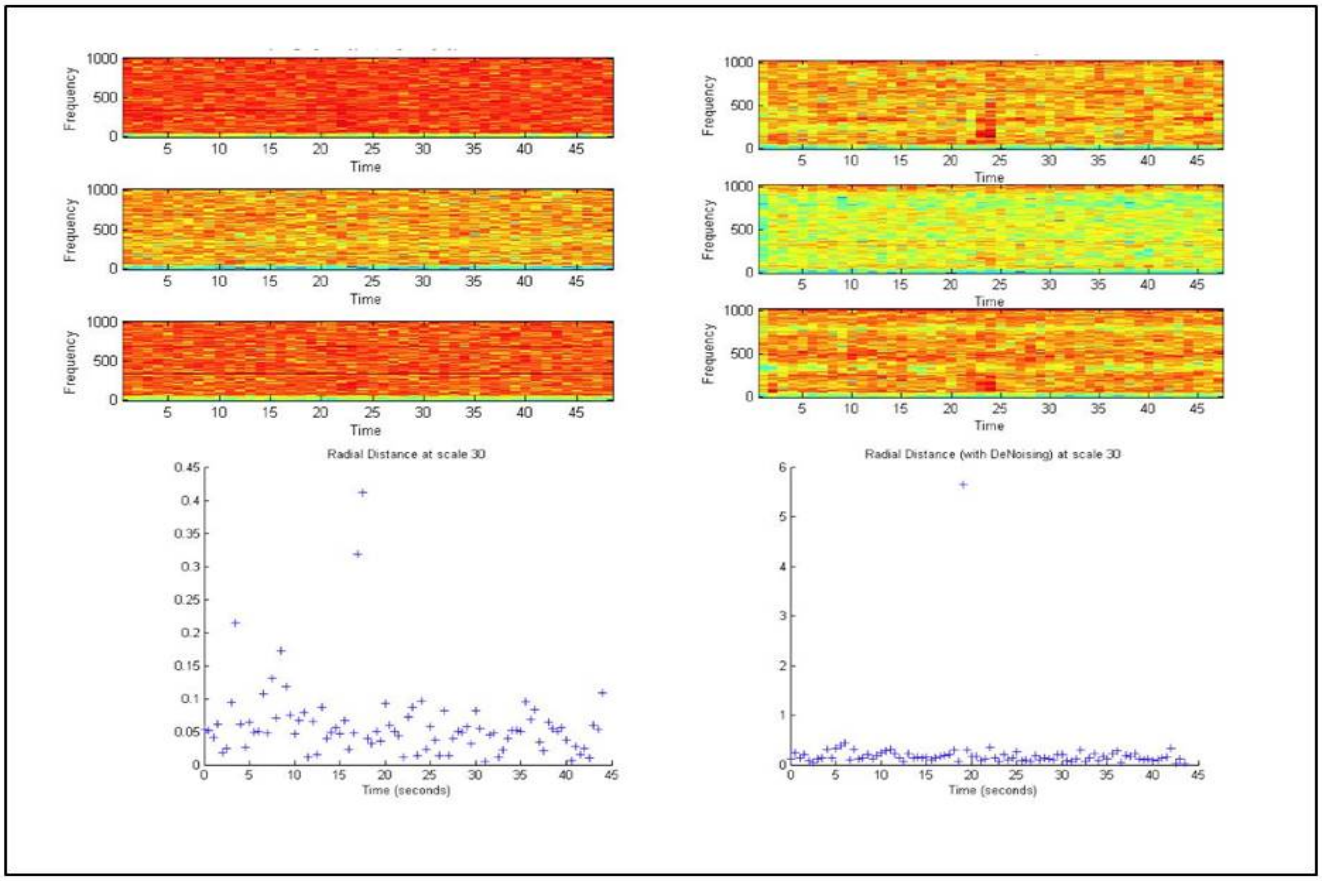

FIG. 5: The figure shows the the spectrograms of the signal (grw_12_2)+noise after being conditioned without the TSNR+HRNR denoising effect (top left panel) and the same with the inclusion of the TSNR+HRNR denoising (top right panel.) The x-axis represents time in seconds and the y-axis represents frequency in Hz. The bottom row of figures shows the radial statistics (as given in equation [36]) for the analysis performed without the proposed denoising (left panel) and with the TSNR+HRNR denoising (right panel.) The x-axis represents time in seconds and the y-axis represents the radial distance.

ysis Volume 32, pp. 531538, 2011

[13] Golub, G. H. and C. F. Van Loan. Sect. 4.7 in Matrix Computations. 3rd ed. Baltimore, MD: Johns Hopkins University Press, 1996.

[14] Gregory M Harry (for the LIGO Scientific Collaboration) Advanced LIGO: the next generation of gravitational wave detectors, Class. Quantum Grav. 27, 2010

[15] S. Mohanty et al, Penalized Likelihood, CQG 23 4799, 2006

[16] M. Rakhmanov, Rank deficiency of network matrix, CQG 23 S673, 2006

[17] Sergei Klimenko, Soumya D. Mohanty, Malik Rakhmanov, Guenakh Mitselmakher, Constraint likelihood analysis for a network of gravitational wave detectors, Phys. Rev. D 72 122002, 2005

[18] Jeremiah W. Murphy, Christian D. Ott, Adam Burrows, A Model for Gravitational Wave Emission in Neutrino-Driven Core-Collapse Supernovae, Astrophysical Journal, 707, 1173, 2009

[19] Bernhard Muller, Hans-Thomas Janka, and Andreas Marek, A New Multidimensional General Relativistic Neutrino Hydrodynamics Code Of Core-Collapse Supernovae. III. Gravitational Wave from supernova emission models, Astrophysical Journal, 766-843, 2013

[20] Yakunin, K. N., Marronetti, P., Mezzacappa, A., et al., CQG, 27, 194005, 2010

[21] Cyril Plapous, Claud Marro and Pascal Scalart, Improved Signal-to-Noise Ratio Estimation for Speech Enhancement, IEEE Transactions on Audio Speech and Language Processing, Vol. 14, 2006

[22] P. Renevey and A. Drygajlo, Detection of reliable features for speech recognition in noisy conditions using a statistical criterion, Proc. Workshop Consistent Reliable Acoust. Cues Sound Anal., Aalborg, Denmark, pp. 71-4, 2001

[23] P. Scalart and J. Vieira Filho, Speech enhancement based on a priori signal to noise estimation, in Proc. IEEE Int. Conf. Acoust., Speech, Signal Process., Atlanta, GA, May 1996, vol. 2, pp. 629632.

[24] Cappe, O., Elimination of the musical noise phenomenon with the Ephraim and Malah noise suppressor. IEEE Trans. Speech Audio Proc. 2 (4), 345349, 1994

[25] Y. Ephram and D. Malah, Speech enhancement using a minimum mean-square error short-time spectral amplitude estimator, IEEE Trans. Acoust., Speech, Signal Process., vol. ASSP-32, no. 6, pp. 11091121, Dec. 1984.

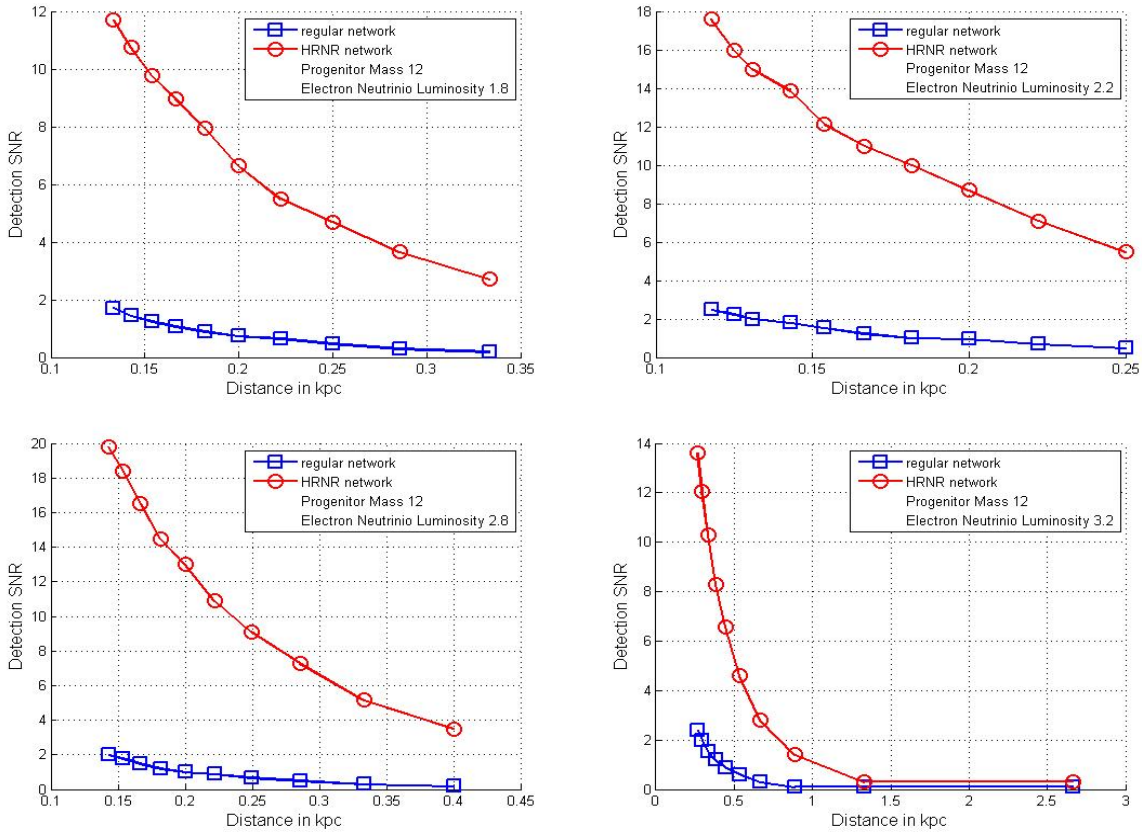

FIG. 6: The figure shows the radial statistics as a function of distance for four waveforms from the catalog. The x-axis represents the distance in kpc. The y-axis represents the detection snr defined from equation [59]. The detection snr is equal to the average value of the radial distance R_{rad} subtracted from the maximum value of the same that corresponds to the event detected. The lower curve (in blue) is the operating characeristic for the original pipeline without the implementation of the proposed TSNR+HRNR denoising module. The upper curve (in red) represents the same with the incorporation of the TSNR+HRNR denoising.

[26] Harry L. Van Trees, Detection, Estimation, and Modulation Theory (parts I and II), Wiley-Interscience; 2001

[27] B. Abbott et al. (LIGO Scientific Collaboration), All-sky search for periodic gravitational waves in LIGO S4 data, Phys. Rev. D 77, 022001, 2008

[28] K. Hayama, S. D. Mohanty, M. Rakhmanov and S. Desai, Coherent network analysis for triggered gravitational wave burst searches, Class. Quantum Grav. 24, 2007.

[29] S. D. Mohanty, Median based line tracker (MBLT): model independent and transient preserving line removal from interferometric data, Class. Quant. Grav. 19, 1513, 2002.

[30] L. S. Finn and S. Mukherjee, Data conditioning for gravitational wave detectors: A Kalman filter for regressing suspension violin modes, Phys. Rev. D 63, 062004, 2001.

[31] A. Sintes and B. F. Schutz,Removing non-stationary, non-harmonic external interference from gravitational wave interferometer data, Phys. Rev. D 60, 062001, 1999.

[32] www.mathworks.com

[33] S. Klimenko, S., I. Yakushin, A. Mercer, et al., Coherent method for detection of gravitational wave bursts , Class.Quant.Grav. 25, 114029, 2008.

[34] N. Wiener, Extrapolation, Interpolation, and Smoothing of Stationary Time Series, New York: Wiley, 1949.

[35] C. Cutler and E. E. Flanagan, Gravitational Waves From Merging Compact Binaries: How Accurately Can One Extract The Binarys Parameters From The Inspiral Wave Form?, Phys. Rev. D 49, 2658, 1994

[36] H. Dimmelmeier, J.A. Font, E. Muller, Relativistic simulations of rotational core collapse II. Collapse dynamics and gravitational radiation, Astron. Astrophys., 393, 523-542, 2002

[37] B. P. Abbott et. al., (LIGO Scientific Collaboration), Observation of gravitational waves from a binary black hole merger, Phys. Rev. Lett., 116, 061102, 2016.

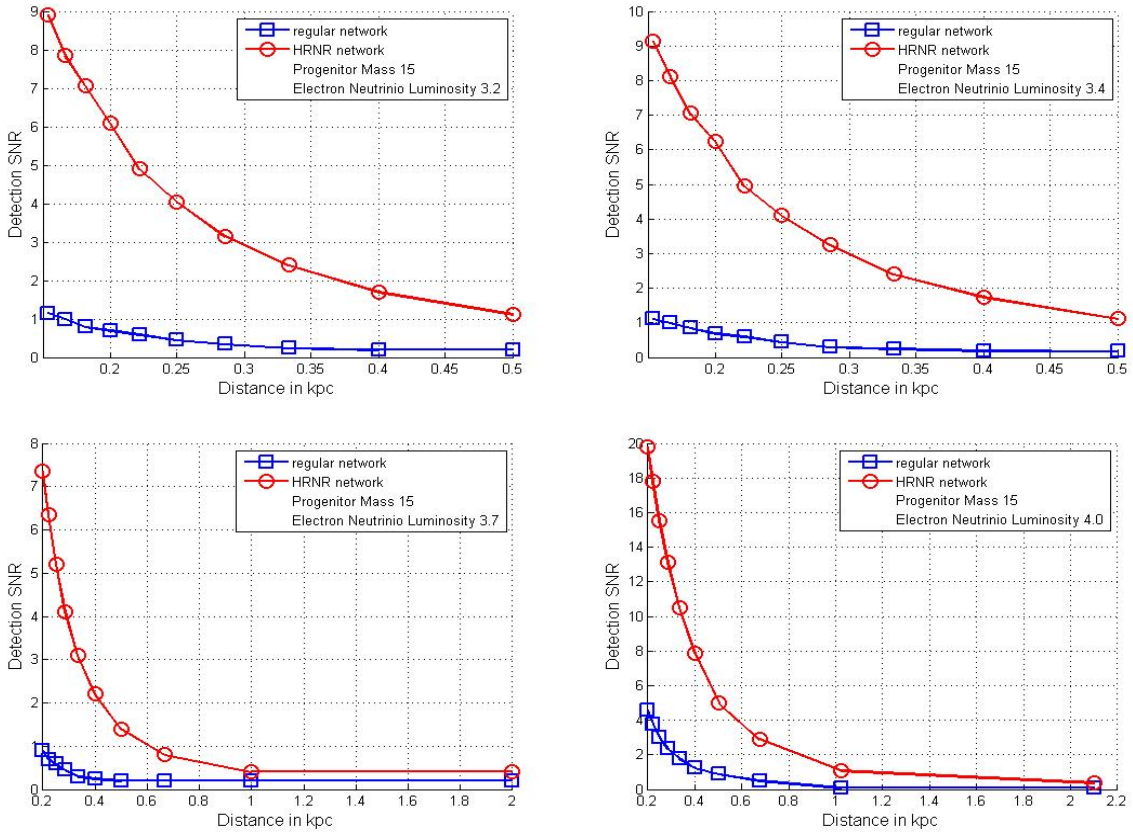

FIG. 7: The figure shows the radial statistics as a function of distance for four waveforms from the catalog. The x-axis represents the distance in kpc. The y-axis represents the detection snr defined from equation [59]. The detection snr is equal to the average value of the radial distance R_{rad} subtracted from the maximum value of the same that corresponds to the event detected. The lower curve (in blue) is the operating characeristic for the original pipeline without the implementation of the proposed TSNR+HRNR denoising module. The upper curve (in red) represents the same with the incorporation of the TSNR+HRNR denoising.

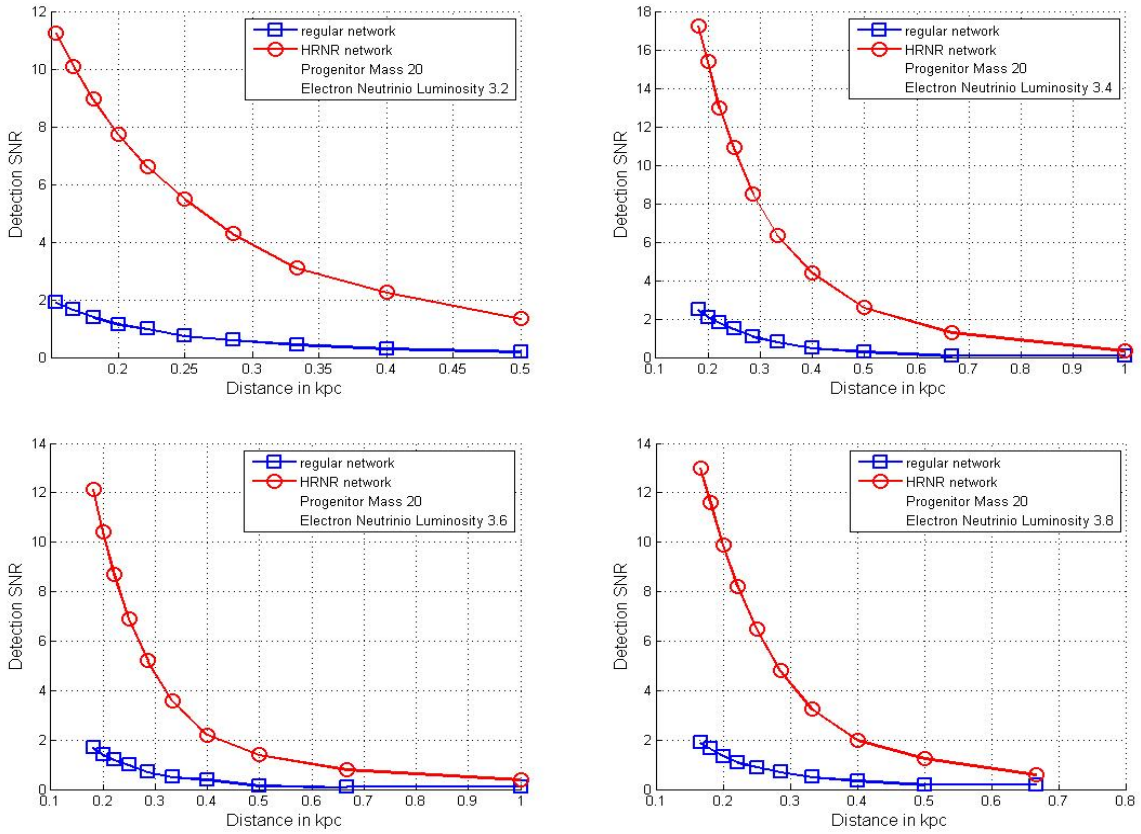

FIG. 8: The figure shows the radial statistics as a function of distance for four waveforms from the catalog. The x-axis represents the distance in kpc. The y-axis represents the detection snr defined from equation [59]. The detection snr is equal to the average value of the radial distance R_{rad} subtracted from the maximum value of the same that corresponds to the event detected. The lower curve (in blue) is the operating characeristic for the original pipeline without the implementation of the proposed TSNR+HRNR denoising module. The upper curve (in red) represents the same with the incorporation of the TSNR+HRNR denoising.

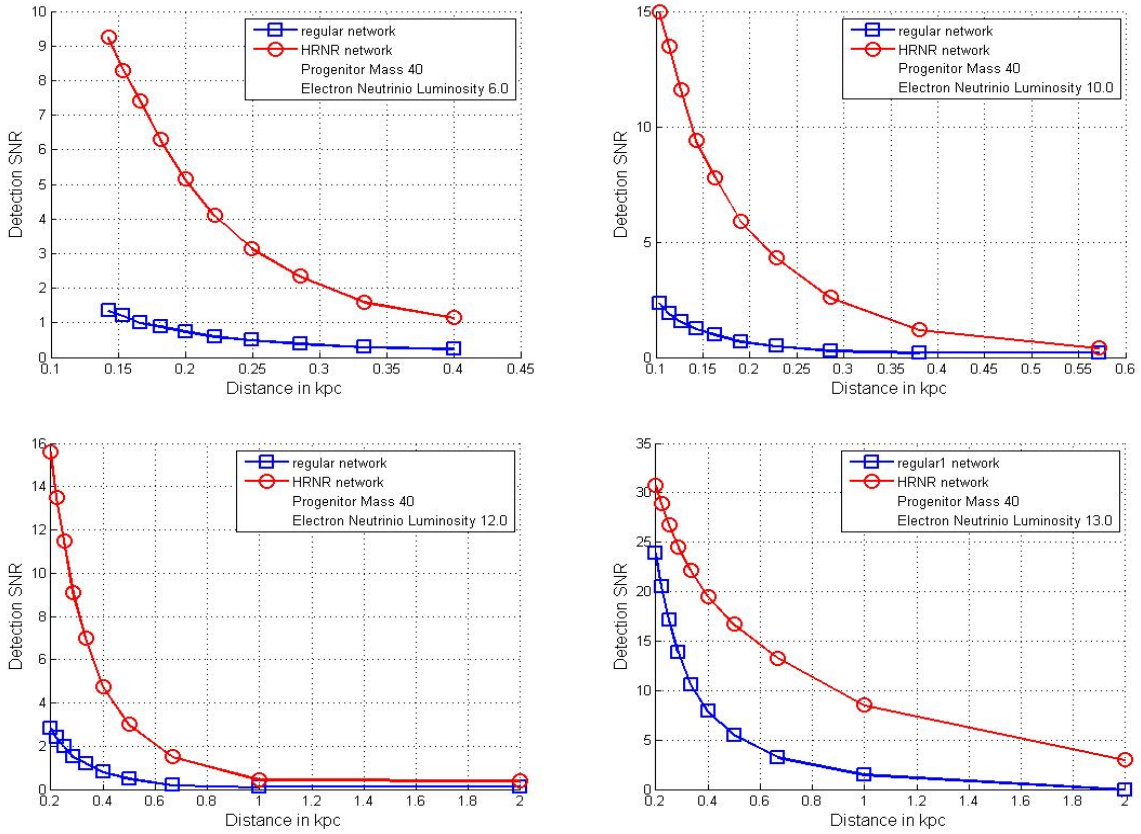

FIG. 9: The figure shows the radial statistics as a function of distance for four waveforms from the catalog. The x-axis represents the distance in kpc. The y-axis represents the detection snr defined from equation [59]. The detection snr is equal to the average value of the radial distance R_{rad} subtracted from the maximum value of the same that corresponds to the event detected. The lower curve (in blue) is the operating characeristic for the original pipeline without the implementation of the proposed TSNR+HRNR denoising module. The upper curve (in red) represents the same with the incorporation of the TSNR+HRNR denoising.